Radial Distribution of the Flow Velocity, Efficiency and Concentration in a Wide HPLC Column

Tivadar Farkas, Michael J. Sepaniak and Georges Guiochon
Department of Chemistry, The University of Tennessee, Knoxville, TN 37996 and Division of Chemical and Analytical Sciences, Oak Ridge National Laboratory, Oak Ridge, TN 37831

The use of optical fibers in a fluorescence-detection scheme permits the accurate determination of the radial distribution of the transit time, the column efficiency, and the analyte concentration at the exit of a chromatographic axial-compression column (50 mmID). The results obtained demonstrate that the column is not homogeneous, but suggest a nearly cylindrical distribution of the packing density. The average velocity close to the column wall is 7% lower than along its axis and the HETP 25% higher. The lack of homogeneity of the column packing is another source of band broadening not taken into account in chromatography so far. It causes the apparent HETP derived from the conventional elution chromatogram recorded on the bulk eluent to be larger than the local HETP and the band profile to be unsymmetrical with a slight tail reminiscent of kinetic tailing.

Introduction

A packed chromatographic column is a maze of channels (i.e., the extra particle pores located between close particles) through which the mobile phase flows. Along the way, it carries those analyte molecules that happen to be dissolved into it. There are countless stream paths along which molecules may migrate from one end of the column to the other. At any given time, the local velocities of molecules following different stream paths or moving at different locations along the same stream path may be very different in magnitude and/or in direction. The flow pattern (i.e., the detailed relative distribution of the mobile phase velocity in magnitude and direction) is a result of all the local velocity biases or differentials that are so important to spreading the analyte zone (Giddings, 1965; Peters et al., 1974). This is the origin of eddy diffusion, which has attracted considerable interest in a variety of other applications. This phenomenon causes most of the apparent axial dispersion observed in high-performance liquid chromatography (HPLC) in the frequent case in which fast mass transfer takes place in the system selected. The proper operation of a chromatographic column requires a narrow distribution of the residence times of the molecules in this column, hence small values of the coefficient of apparent axial dispersion.

Correspondence concerning this article should be addressed to G. Guichon.

There are a considerable number of publications on hydrodynamic dispersion that cannot be reviewed comprehensively in this work. The chromatographic literature relevant to this issue has been discussed recently (Tallarek et al., 1997). The major contributions of Ebach and White (1958), Gunn (1968, 1969), and Hiby (1962) must be acknowledged. These authors have derived correlations between the axial and radial Peclet numbers and the Reynolds number. However, all of this previous work was performed under such experimental conditions that the Reynolds number exceeds 0.10. By contrast, liquid chromatography is carried out at such low average mobile phase velocities that the Reynolds number is of the order of 1×10^{-3}, that is, undoubtedly under strict conditions of so-called *creeping flow*. The best correlation found between particle Peclet number and apparent axial dispersion in chromatography was the Giddings equation [Tallarek et al., 1997]. In this last work, however, the dispersion coefficients were measured from pulsed field gradient nuclear magnetic resonance (PFGNMR) signals. Thus, they result from the amount of dispersion undergone by all the molecules contained in the column during a short period of time (less than 100 ms). It is not surprising, then, that the dispersion coefficient derived from the width of the residence time distribution is much larger (Tallarek et al., 1997), since the latter includes a contribution arising from the large-scale fluctuations of the mo-

bile phase velocity (averaged over a distance of a few particle diameters). Any such fluctuation would warp the band profile, causing the locus of the maxima of the concentration profiles along straight lines parallel to the column axis to differ significantly from the plane. This warping of bands during their migration along a column has been reported conclusively by NMR imaging of bands of Gadolinium chelates (Tallarek et al., 1995; Bayer et al., 1995).

Most authors of basic references on fluid dynamics in porous media, and more particularly in chromatography (Giddings, 1965), consider a thorough treatment of microscale flow patterns in packed beds [see the discussions of so-called *capillaric models* of packed beds by Collins (1961) and Scheidegger (1974)], but give only rather evasive descriptions of the overall flow profile over the column cross section. Chromatographers still tend to consider the network of channels in a column as a bunch of interconnected capillary tubes in each of which Poiseuille law would apply (Karger et al., 1973; Poole and Poole, 1993). This view is untenable, however, as the channels are not cylindrical and are no longer than they are wide. Furthermore, conventional wisdom has it that, overall, the flow profile in packed beds is flat and, so far, all studies, theoretical as well as experimental, have assumed that the columns are radially homogeneous and that only one spacial dimension is needed in any realistic chromatographic model. However, there is now incontrovertible evidence that the beds of chromatographic columns used in analytical applications do not experience an even flow velocity over their entire cross section (Baur et al., 1988, Baur and Wightman, 1989; Eon, 1978; Farkas et al., 1994, 1996; Horne et al., 1966; Knox et al., 1976). On the contrary, there is a significant, columnwide variation in the value of the average velocity along the many tortuous stream paths that run more or less parallel to the column axis.

All the experimental results just cited and that regard the homogeneity of column packings and the radial distribution of the flow velocity, column efficiency, and solute concentration, have been obtained using analytical-size columns (4.6 mm i.d.). Recent qualitative results by Kamiński (1992), who used dyes to visualize band profiles inside 17 to 52-mm-ID columns, suggest that most packed columns are heterogeneous. Because column heterogeneity seems to be related to the influence of the wall on the consolidation of the bed, it is still not known whether the same effects take place in larger diameter columns used for preparative applications of chromatography. It would be of great practical importance to determine whether the "wall effect," first identified by Knox (Knox et al., 1976; Knox and Parcher, 1969) extends over a constant distance [e.g., 50 particle diameters, as suggested by Knox et al. (1976), and confirmed by Eon (1978), and Baur et al. (1988, 1989)] or over a constant fraction of the column diameter. The consequences for the performance of a wide bore preparative column would be serious. The goal of this work is to investigate the degree of homogeneity of such a preparative size column and to ascertain how many spatial dimensions are required for the proper modeling of chromatographic columns: one, as used by nearly all specialists (Guiochon et al., 1994); two, as recently suggested by Yun and Guiochon (1994, 1996); or three, as would be needed in the worst of cases. For this study, we have combined the methods previously developed in our laboratory for the preparation of efficient preparative columns by dynamic axial compression (Sarker and Guiochon, 1995a,b; Sarker et al., 1996) and for the local measurement of the concentration histories during chromatographic experiments with analytical columns (Farkas et al., 1994, 1996).

Experimental

This work consists of recording simultaneously the concentration histories upon elution of a chromatographic band in a number of different locations in the exit cross section of the column and of comparing the characteristics of the profiles obtained. Fluid dynamics suggests that the local perturbations of the flow pattern caused by the presence of the probes or concentration sensors in a packed medium take place well behind the tip of the probes while the concentrations are measured at the probe tip (microelectrodes in an electrochemical detector, Farkas et al., 1994) or in a volume slightly ahead of the probe tip (spectrofluorescence with optical fibers, Farkas et al., 1996). At the very low Reynolds number achieved, there is no local turbulence and backward flow at a scale larger than the fiber tip size is not possible.

Both electrochemical and optical methods gave the same results with analytical-size columns, but the second one turned out to be more practical (Farkas et al., 1996). Accordingly, the latter method was used in the work reported here. Local, on-column detection is easier to implement with preparative-scale columns than with analytical-size ones. Spatial constraints are less stringent in the former than in the latter case. Bulkier, sturdier sensors can be used. The number of sensors that can be placed in the outlet cross section of the column is larger. At the same time, however, the ratio between the volume element of the column sampled by a specific microdetector and the overall volume to be investigated (the component zone) is much smaller in the case of preparative columns than in the case of the previously investigated analytical-size columns (Farkas et al., 1994, 1996). This makes the implementation of a large number of detection units necessary. In practice, this number is limited only by the number of parallel channels on which detection can be performed simultaneously.

The diode array detector (DAD) used in the experiments reported here has 35 photosensitive diodes. Not all these diodes can be used as parallel detectors because of optical cross talk caused by the light scattering that takes place in the small volume situated between the very end of an emission optical fiber and the surface of the diode the fiber is shining its light on. Because of this scattering, part of the fluorescence collected by a given fiber also reached the diodes situated on either side of the primarily targeted diode. For this reason, only every second diode was targeted, with fibers arranged accordingly. Furthermore, a proper arrangement of the sequence in which the different locations investigated within the column outlet cross section were connected to the elements of the diode array facilitated accounting for any possible optical cross talk. Every photosensitive diode integrated the light shone onto it without discriminating between the light brought by the fiber centered onto it and the scattered light coming from neighbor fibers. For this reason it was important either to check that the amount of scattered light was small at the level of a particular diode, or to ensure

a sufficient shift in time between the detection of the light coming from two different sources. The way to do this was to ensure that the two adjacent parallel channels were always connected to sensors giving signals exhibiting important or considerable difference in their retention time. Then the effect of the optical cross talk between the channels results in small parasite peaks seconding the actual peak recorded on the specific diode. This small peak precedes or follows the main peak, depending on the case. At the same time, its characteristics match those of the peak recorded on the channel where the scatter took place, and hence can be checked for self-consistency. This eliminates peak shape distortion caused by differences in optical response and/or electronic signal manipulation at a specific diode level. Diode calibration is carried out through a series of breakthrough curves (see below).

Detection system

The instrumental setup is similar to one previously described (Farkas et al. 1996) using analytical scale columns (Figure 1). The beam of an argon-ion laser is directed through a bundle of optical fibers (excitation fibers) to selected locations at the column outlet. Each excitation fiber is mated to an emission fiber that collects the emitted fluorescence of a laser dye (used as the analyte) in the immediate vicinity of the excitation fiber, and transmits it to a diode-array detector. The collected light is shone onto the appropriate pixel of the DAD and translated into an electrical signal which is acquired and stored by a microcomputer.

The argon-ion laser (Model INNOVA 100-15, Palo Alto, CA) was operated at 488 nm. The estimated power at the sensing side of the optical fibers was 800 mW. When operated at a higher power (1.0 W), the jacket of the optical fibers at their end facing the laser beam became charred. The optical fiber assemblies were made in the same way as described previously (Farkas et al., 1996), using quartz fibers (P/N: 16-0105-HAS-C22 of General Fiber Optics, Cedar Grove, NJ) with a core diameter of 105 μm.

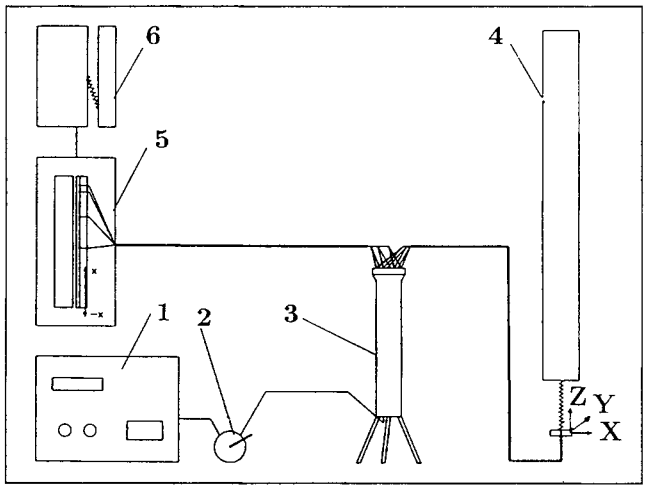

Figure 1. Instrumental setup for on-column fluorescence detection using optical fibers on an axial compression LC-50 preparative column.

1. HPLC pump; 2. injection valve; 3. LC-50 preparative chromatography column; 4. Ar laser; 5. photodiode-array detector; 6. IBM PC.

Few adjustments had to be made in order to accommodate the large-size column. The length of the optical fibers was increased from 0.9 m to about 1.5 m. The length of the metal sheath holding and protecting the uncovered fiber cores was increased to about 7 mm, to permit its easy penetration through the outlet frit of the preparative column used (see below). This frit is much thicker than the frits used with analytical-size columns (5 mm vs. 1.575 mm). The joint reinforcement of each optical fiber assembly was increased in volume in order to confer more mechanical resistance to the joint. This was necessary because the larger spacing between the different assemblies used prevented increasing their mechanical resistance by bonding them into a bundle, as was previously done (Farkas et al., 1996). Arranged in this manner, each fiber couple probed a region in the frit less than 0.5 mm in diameter, to a depth of less than 0.5 mm.

Calibration of the fibers is carried out by running breakthrough curves. The advantage of frontal analysis over elution for these studies is that, even if the packing is heterogeneous, the composition of the whole effluent eventually becomes homogeneous, given enough run time. The ratio of the steady-state signal heights measured at different locations over the column cross section vs. the one recorded at column center was used as a correction factor for the differences in the fiber-assembly responses.

Liquid chromatography system

The chromatographic system consisted of a DYNAMAX (RAININ Instruments Co., Woburn, MA) Solvent Delivery System Model SD-1 with a maximum flow rate of 800 mL/min; a 50-mmID LC-50 Axial Compression Column skid (PROCHROM, Indianapolis, IN), and a LINEAR (Linear Instruments, Fremont, CA) UVIS 204 absorbance detector. This detector was used only for testing the columns after packing them, in order to follow the progressive stabilization of their bed and make sure that the beds studied were those of typical, efficient columns (Sarker and Guiochon, 1995a,b). The column skid was described previously (Sarker and Guiochon, 1995a). It allows the packing of columns up to 300 mm long, axially compressed under a mechanical stress with a maximum value of 100 kg/cm^2, and can be operated under an inlet pressure up to 150 atm.

The chromatographic column was slurry packed using a suspension of 270 g of ZORBAX PRO-10/150 C_{18} bonded spherical silica (BTR Separations, Wilmington, DE) in 800 mL of 2-propanol. The average particle size is 10 μm, and the average pore size is 150Å. Further details regarding the physical properties of these particles are available elsewhere (Guan et al., 1996). The slurry was treated by ultrasonication for 5 min prior to being poured into the open column, after which the outlet frit was put in place, the outlet flange bolted, and proper axial compression stress applied without flow. The liquid exiting the column was collected and its volume measured (Sarker and Guiochon, 1995b). The oil-gauge reading during column packing was 110 bar, which translates into an average stress applied by the piston to the top of the packing of approximately 45 kg/cm^2. The phenomena observed during consolidation of the bed were described and discussed previously (Guiochon and Sarker, 1995; Sarker et al., 1996). After stabilization of the packing, methanol was run through

the column for 2 h at a flow rate of 50 mL/min to promote bed stabilization (Sarker and Guiochon, 1995a,b). Subsequently, the column was tested with methanol at the mobile phase, at a flow rate of 50 ml/min. Three different solutes were used as test samples: 0.4 g/L uracil, 0.4 g/L 4,5-dibromofluorescein, and 0.35 g/L disodium fluorescein (disodium salt of 3′,6′-dihydroxyspiro[isobenzofuran-1(3H),9′-[9H]xanthen]-]-one), with the UV-VIS absorbance detector set at 254 nm for the first solute and 488 nm for the other two. The last compound is the fluorescent species used for local detection. With a molecular weight of 332.30 dalton, it has a low diffusivity. This explains the high values of the reduced velocity achieved and the low transverse dispersion coefficient obtained (see later).

Two columns packed following the same procedure were investigated. Both columns were 50 mm in inner diameter and approximately 150 mm long. The packing used for the first column was recovered and reused for packing the second column. The column was open, the packing cake pushed out of the cylinder by raising the piston, and the cake was suspended in the proper amount of solvent by ultrasonication. As shown later, in the section on column efficiency, recycling the packing did not negatively affect the performance of the second column. This result is in agreement with previous observations made on ZORBAX (Sarker and Guiochon, 1995a; Sarker et al., 1996), but is not valid for all packing materials (Sarker et al., 1996). These two columns exhibited the same properties as previously reported (Sarker and Guiochon, 1995a,b; Sarker et al., 1996) and were considered as representative, and hence useful for further study.

After testing the column, its top flange and frit were carefully removed and replaced with a modified flange that embraced a new frit holding eleven optical-fiber assemblies (Figure 2). These assemblies were positioned in the outlet cross section of the column in such a way that measurements of the elution profiles (this term has become so conventional in the chromatographic literature that it is difficult to avoid it systematically; still, it is a misnomer, as it means, in fact, a concentration history) were carried out at different, well-spaced values of reduced column radius, along two perpendicular directions (Figure 2). New measurements were carried out after successive rotations of the holding frit by steps of 90° angle around the column axis. This allowed most fibers to relocate between points in which measurements had been carried out in the previous position and a few others in points in which measurements had been done previously. This allowed confirmation of these previous measurements by revisiting the same site with other fiber assemblies during different runs and by permitting checks for self-consistency of the results.

The sample selected for on-column detection (Farkas et al., 1996) was 1.15×10^{-3}-M Disodium Fluorescein (a laser dye with a good quantum yield, purchased from Exciton, Dayton, OH) dissolved in 40% methanol + 60% water. The sample solvent had the same composition as the mobile phase. A six-position VALCO injection valve operated by an electric actuator (VICI, VALCO Instrument Co., Inc.) and having a 0.5-mL sample loop was used for each run.

Determination of the injection profile

To determine the actual injection profile in an analytical

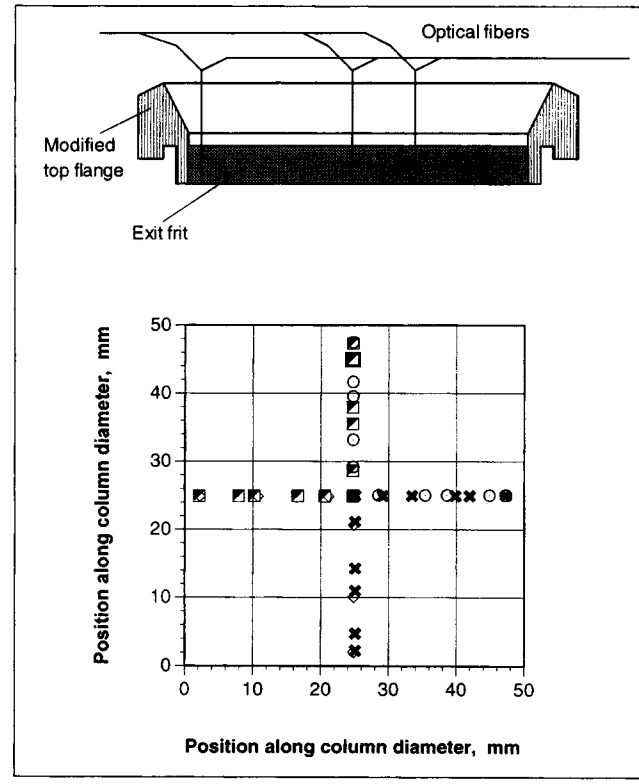

Figure 2. Modified top flange with exit frit holding optical-fiber assemblies and locations investigated over the column exit cross section.

column (Farkas et al., 1996), the column was removed and the local, on-column detection system was attached next to the inlet frit, above the injection distributor disk that comes with most analytical-size (4.6-mm-ID) columns. In this manner, the profiles recorded at column inlet are not typical of a specific analytical size column, but of the injection system used. Our system was made of an injection valve (Rheodyne Model 7010), a 20-μL injection loop, a common inlet fitting (Parker), and connecting tubing. The results obtained with this experimental setup showed that the front and rear borders of an injection plug are rapidly eroded during and after injection, during the transfer of the band inside the loop of the sampling valve, through the tubing connecting this valve with the column inlet, and through the inlet fitting itself. This fast decay is caused mainly by convection and also by molecular diffusion along the concentration gradients. The passage of the analyte band through the inlet frit did result in narrow peaks that were nearly simultaneous and very similar in shape (Farkas et al., 1994). This means that the plug of analyte molecules entered the chromatographic column as a flat, radially homogeneous band and that the thickness of this band in the axial direction contributed to a negligible extent to the width of the band exiting the column. Consequently, any distortion registered at the column outlet was caused by the inhomogeneous bed structure.

In the case of the preparative column, the large size of the cross-section area allows a simpler and clearer determination of the distribution of the concentration density of the feed sample at column inlet. A sample of the silica used in the other experiments reported here was impregnated with a

small amount of sodium hydroxide (in a methanol solution). The column was packed in the conventional way, using a methanol slurry of this modified silica. The thickness of the packing layer obtained was approximately 7 mm. The column was operated with pure methanol at 25 mL/min. After one minute, an injection of 0.5 mL of a 1-mM acetic acid solution in methanol was performed and the methanol flow was stopped after another minute. The packing bed was extruded from the column, cut with a cookie cutter, and partitioned into four circular sectors and 12 regions (Figure 3), which were all removed and collected in separate vials. These 12 fractions were titrated for the amount of sodium hydroxide remaining per gram of the packing material. Each vial was dried to constant weight (which causes the silica to agglomerate tightly), treated with a solution of 0.01-N hydrochloric acid solution (in excess), and the unreacted acid was back-titrated with a solution of sodium hydroxide in the presence of phenolphthalein.

Sodium hydroxide reacts with silica and forms sodium silicate. The amount used here is insufficient to cause dissolution in methanol; only ion exchange takes place upon reaction with acetic acid. Although the solubility of sodium hydroxide in methanol is far from negligible (0.21 g/mL), no significant extraction by methanol takes place during the experiment, as confirmed by a blank experiment. Back titration is required, however, because sodium hydroxide is released too slowly from the agglomerated dry silica during a conventional titration. The sodium acetate does not affect the result of the titration of a strong base in the presence of phenolphthalein. The results are shown in Table I. They demonstrate that after injection of the acid sample, the sodium hydroxide content of the treated silica was constant over the entire cross-section area of the column (relative standard deviation for the 12 fractions, 1.34%). This proves an even radial distribution of the concentration of the injected sample at the inlet of the preparative column, that is, a flat injection profile.

Results and Discussion

Radial distribution of the mobile phase flow velocity

Considering that most of the chromatographic bed in a preparative column undergoes sedimentation in a volume that is located far from the column wall, it would seem that a nearly homogeneous bed should be expected. Compared to the flow velocity distribution at the outlet of an analytical-size column, the corresponding distribution in a preparative column should have a much flatter profile.

Contrary to this rationale, the results of a few simple experiments carried out recently by Yun and Guiochon (1997) suggest that there is a "wall effect" that is real and extends far from the wall, even in the case of large-diameter columns. In one of these experiments, a dye was injected into the same axial compression column as the one used here and eluted under conditions in which the dye retention factor is small. The elution was stopped when the dye had moved nearly halfway through the column by switching off the pump. The column was then opened, the bed of packing material was pushed out of the column and recovered as a cake, which was cut along its longitudinal axis. Examination of the section showed that the dye zone was not flat. Its profile was more like that of a fourth- or sixth-degree polynomial centered on

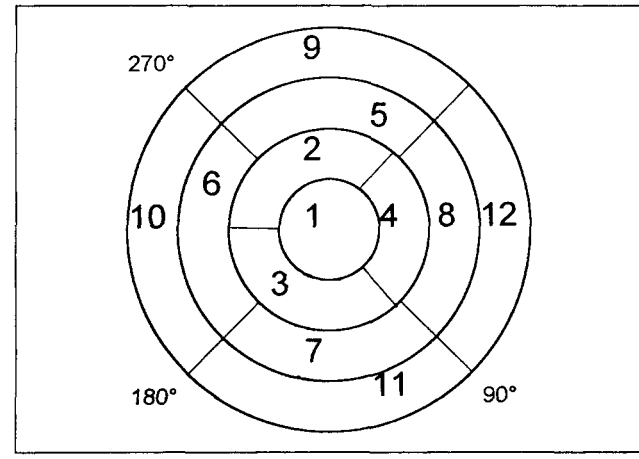

Figure 3. Fractionation of the layer of NaOH-modified silica for determining the concentration distribution at feed injection.

the column axis, nearly flat in the central region up to approximately two-thirds of the column radius away from the column axis. In the external region, along the column wall, the dye zone curves slowly toward the column inlet, demonstrating that the local mobile phase velocity decreases from the center toward the column wall. Molecules propagating in this annular region (which accounts for approximately half of the column volume) elute markedly later, the local velocity close to the wall being 13% lower than in the column center (Yun and Guiochon, 1997).

The results obtained in this study and reported here underscore this description. Figure 4a and 4b show the distribution of the relative linear velocity difference $(u - u_c)/u_c$ (in %), between the velocity, u, at locations along two different, perpendicular column diameters and the velocity, u_c, at the center of the outlet column cross section, taken as the reference. The values for the local linear velocity plotted in Figure 4a and 4b were calculated as the ratio between the length of the column and the local value of the residence time of the band maximum recorded at the radial location of interest. The reference point—$(u\text{-}u_c)/u_c = 0$, for $u = u_c$—is marked in Figure 4b by the solid line dropped to the XY plane. The z coordinate of this point—as of any other point in the

Table 1. Uniformity of the Injection Band over the Column Cross Section

Sector No.	Wt. of Sample Collected	mmol of NaOH/ g of Sample
1	0.1843	0.667
2	0.4271	0.681
3	0.3579	0.660
4	0.4305	0.660
5	0.6832	0.661
6	0.8866	0.658
7	0.8945	0.671
8	0.8452	0.686
9	1.2055	0.656
10	1.0659	0.670
11	0.9616	0.670
12	0.8925	0.664
	Avg. NaOH lod (RSD)	0.667 ($\sigma_{n-1} = 1.34\%$)

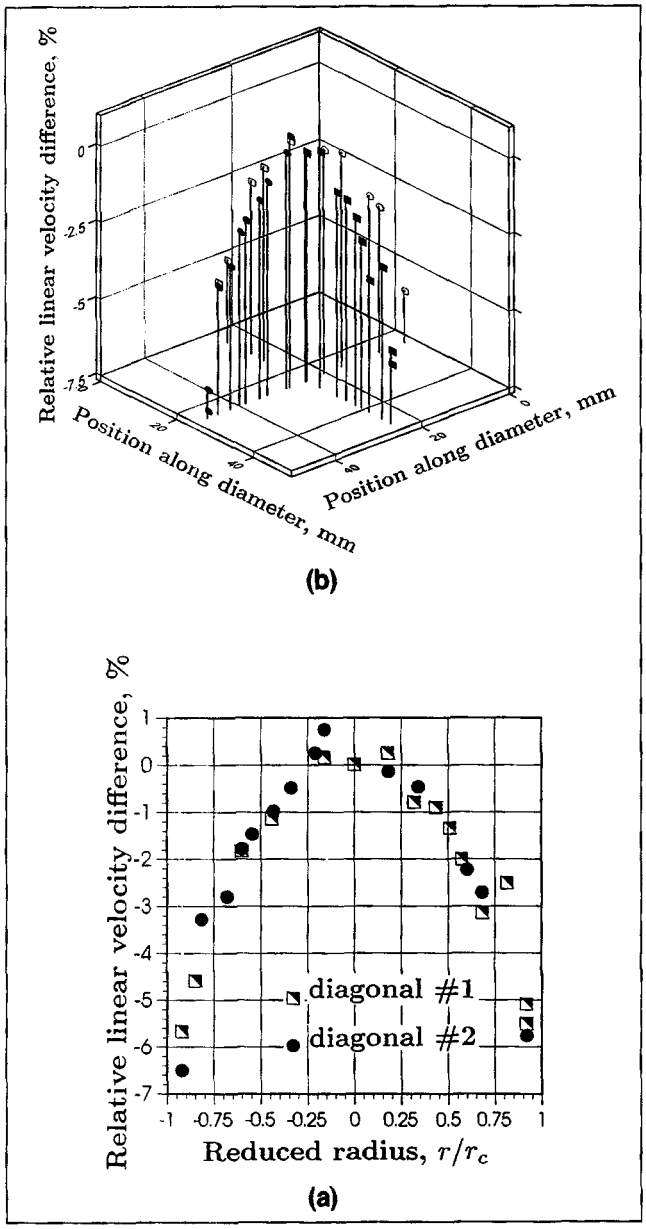

Figure 4. Distribution of the mobile phase velocity at the column outlet.

Plots of the relative linear velocity difference vs. the radial position. (*a*) 3-D view of the mobile phase velocity distribution along two perpendicular diameters for a 50 mm×150 mm Zorbax PRO-10/150 C_{18} spherical silica column; particle size 10 μm; open symbols were adopted for data measured at locations of detection situated behind the viewing angle. (*b*) 2-D view of the same distribution along the two individual diameters, overlaid.

plot—can be determined by projecting the line dropped from the point to the *XY* plane onto the *z*-axis.

The most obvious characteristic of the velocity profiles presented in Figure 4a and 4b is their near cylindrical symmetry. It is obvious that there is a large difference between the linear velocity in the core region and that in the wall region of a preparative-scale chromatographic column. The linear velocity appears to be highest at the column axis. The profile of the velocity distribution is flat around the column center and decays rapidly close to the column wall. This decay seems to be continuous, with no discontinuity.

It has been a recurring observation (Farkas et al., 1994, 1996) that the analyte retention time measured in efficient analytical-size columns at locations between one-third and one-half of the column radius away from the column center tends to be slightly shorter than the retention time recorded at the very center of the column. This finding suggests that there may be an annular region around the axis of efficient columns where the flow is the fastest, while the flow in the central region would somewhat lag behind (generally by no more than 1%, often by less than 0.5%). This result is illustrated in Figure 5, which shows the overlaid plots of the relative velocity differences as a function of the radial position of the probe for three different 4.6-mm-ID columns. Many experiments made on larger columns suggested the same pattern, although a definitive conclusion cannot be drawn. The reason for this is that too few data points were acquired in the vicinity of the column center because the column is large and we could not afford the density of data points around its center that would have been required, without losing more important information close to the column wall. The precision of our measurements (the relative standard deviation is less than 3.5% for 6 to 8 consecutive runs) precludes any doubt regarding the prevalence of locations around the column axis, where the linear velocity is higher than at the column center. At the same time, however, measurements made at different locations corresponding to the same radius (i.e., along a circle centered at the column axis) also resulted in some data points contradicting this observation. Mapping out this region of the packing would have required placing all of the fiber assemblies close to the column center.

A probable explanation for these results would be that the profile of the flow velocity distribution in the core region of the bed is not flat but wavy. The reference sensor located at the column center could be only by chance (i.e., rarely) lo-

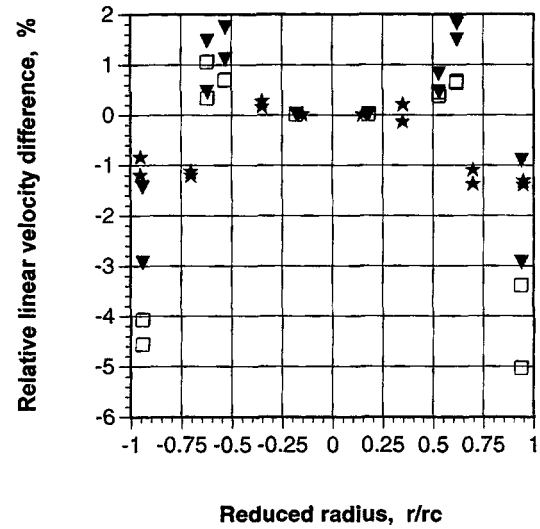

Figure 5. Distribution of the mobile phase velocity at the outlet of three different analytical columns.

Relative linear velocity difference vs. relative radial position. □, 4.6-mm×200-mm column, packed with 10-μm silica particles; ●, 4.6-mm×150-mm column, packed with 16-μm silica particles; ★, 4.6 mm×100 mm-column, packed with 10-μm silica particles.

cated at the top of a wave; most often, the velocity in many locations around the center would be faster, but in some places it would be lower and the cylindrical symmetry would be lost for this feature. This explanation is in agreement with the results of the observations of the profiles of zones of gadolinium complexes reported recently by Tallarek et al. (1995) and Bayer et al. (1995). Anyway, the velocity differences measured in the core region of the bed are much smaller, and consequently much less important, than the important decrease of the velocity in the wall region.

The linear velocity, u, of a viscous fluid percolating through a packed bed under a pressure difference, ΔP, is given by Darcy's law:

$$u = \frac{k_o d_P^2 \Delta P}{\eta L}, \tag{1}$$

where η is the viscosity of the fluid, d_p is the average particle size of the packing material, L is the column length, and $k_0 d_p^2$ is the permeability of the bed. Since pressure is transmitted evenly through fluids, the same pressure drop drives the fluid through the packed bed along each stream path. The local value of the bed permeability determines the corresponding value of the linear fluid velocity. Ideally, the packing of a chromatographic column should be homogeneous, showing an even value of the permeability throughout its volume. Experimentally, the radial and axial distribution of the permeability is very difficult to determine. Our experimental results suggest that there is a systematic variation of the local permeability in the radial direction. According to Darcy's law, the regions of high packing density (i.e., of low permeability) should experience a slower flow than the regions of low packing density, under the same pressure gradient. Since the flow-rate distribution at the column outlet (Figures 4a and 4b) indicates that the linear velocity is maximum at the column center and becomes smaller as the point of detection is moved from column axis to column wall, the local packing density should increase with increasing reduced radial distance. In the regions where the permeability is high and the pressure gradient small, however, the local flow rate does not depend on the local permeability. There the local velocity is inversely proportional to the local value of the external porosity. Such regions seem to exist, at least in certain chromatographic columns.

The packing heterogeneity described in the previous paragraph is related to the relatively high compressibility of pulverulent materials (Taylor, 1948; Sarker et al., 1996) and to the complex distribution of stress during the compression of the packing. Train (Train, 1956, 1957; Train and Hearsey, 1960) has shown that the distribution of stress in a powder mass during its axial compression inside a cylindrical die is far from uniform. For example, under compression stress equivalent to 45 kg/cm^2 applied to the piston located at the top of a 53-mm×145-mm die, the local stress at the end of the bed opposite to the piston was approximately 15 kg/cm^2. It was 20 kg/cm^2 both in the geometrical center of the bed and against the center of the piston. The local stress against the piston increased with increasing distance from the piston center toward the die wall. The highest local stress measured was slighty higher than 50 kg/cm^2, in the region close to both the die wall and the piston (Train, 1957). The packing density was higher in the regions of higher stress. So, it should not be surprising that the packing of a chromatographic bed obtained by axial compression is heterogeneous, and that its regions of higher packing density (lower permeability) experience a lower linear velocity.

Column efficiency

The column efficiency was determined using the conventional relationship

$$N = 5.54 \times \left(\frac{t_r}{W_{1/2}} \right)^2, \tag{2}$$

where N is the number of theoretical plate; t_r the retention time of the test analyte; and $w_{1/2}$ the peak width at half height. In Figure 6 the local reduced HETP, $h = L/(N d_p)$, is plotted against the reduced radius of the column. The data obtained with two different columns are overlaid. The plots in Figure 6 prove that the local column efficiency varies systematically along the column diameter. The lowest values of the local reduced HETP ($h = 3.9$) for the first column investigated in this study (square symbols) were recorded at locations close to the column center, while the highest values ($h = 5.1$) were found close to the column wall. The same trend was observed with the second, slightly more efficient column, which also exhibits a reduced HETP more than 30% larger close to the column wall than in its center. The values of the local HETP ($h = 3.9$ to 5.1 for the first column, 3.1 to 4.4 for the second) must be compared to the average plate height measured for the same columns in a classic instrument setup, using an online detector on the bulk outlet stream of mobile phase. Uracil, 4,5-dibromofluorescein, and disodium fluorescein, all at a concentration of 0.4 g/L, were used for this purpose. At the same mobile phase flow rate as before (50 mL/min), values of the reduced HETP of 7.2, 6.9, and 8.7 were found for

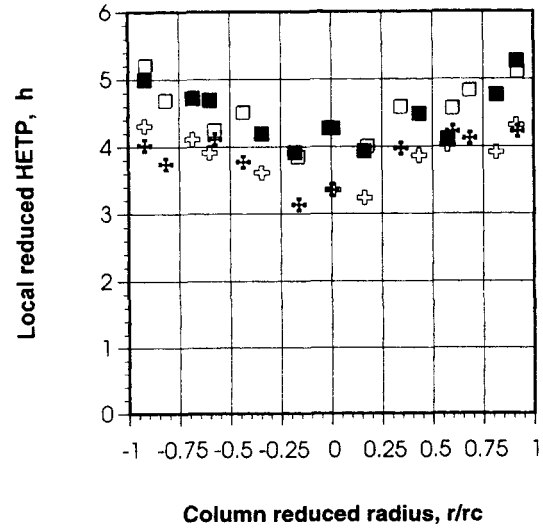

Figure 6. Distribution of the local column efficiency along the column diameter for two axial compression columns investigated, overlaid.

■ and □ local efficiency for column 1 along two perpendicular diameters; ✣ and ✣ corresponding data for column 2.

uracil (retention factor, $\kappa' = 0.1$; reduced velocity, $\upsilon = 11.8$), Dibromofluorescein ($k' = 0.88$, $\nu = 27.7$), and disodium fluorescein ($k' = 0$; $= 18.6$). These average or apparent values are larger than any of the local reduced HETP recorded.

These results are explained by the radial distribution of the mobile phase velocity, which causes an early elution of the core region of the band and a late elution of its peripheral region. As a consequence, local, on-column detection always results in narrower peaks, exhibiting less tailing and a band shape closer to a Gaussian profile, even if the local efficiency were to be constant, independent of the radial position. This result is in agreement with the independent findings of Baumeister et al. (1995) and Tallarek et al. (1997), who used pulsed field gradient NMR to measure the average axial dispersion coefficient in the column at a given time and found it much lower than the value derived from the chromatograms recorded by an on-line detector.

These results illustrate the observation made long ago by Giddings (1963) that trans-column variations of the mobile phase velocity have pernicious effects on the column efficiency. The distribution of the flow velocity inside a chromatographic column has a considerable influence on the outcome of an analysis or a preparative separation. A 5% difference between the velocities in the column center and close to its wall means that when molecules of the second component of a binary mixture with a separation factor of 1.05 leave the column center, they coelute with those molecules of the first component that migrated close to the column wall. Radial dispersion can relax the corresponding concentration gradients in a narrow-bore analytical column (ID less than 0.5 to 1 mm). They cannot do so in a preparative column (Knox and Parcher, 1969). It is only if the distribution of the population density of the analyte molecules follows a narrow normal distribution along the column axis with a mean position and a variance independent of the radius that we obtain the narrow and symmetrical peaks required for the achievement of highly efficient separations. Any distortion of this ideal structure of the analyte zone results in dramatic loss of column efficiency. Such a loss takes place when the mobile phase propagates along the column with a radial velocity profile that is not flat.

It is important to realize that, although the effects are illustrated in this work by data obtained with weakly retained analytes ($k' = 0.88$ or lower), the influence of a radial distribution of the liquid-phase velocity is independent of the retention. The propagation velocity of a chromatographic zone under linear conditions is $\upsilon = u/(1+k')$, hence it is proportional to the liquid-phase velocity, whatever the retention. Under nonlinear conditions, the velocity associated with a concentration is also proportional to u. Thus, any radial distribution of the liquid-phase velocity will cause a proportional distribution of the analyte velocities. These results are applicable to solutes with retention factors much larger than unity. This conclusion had already been reached by Knox and Parcher (1969). As was shown by Giddings (1965), the column HETP is the sum of contributions originating from different, independent sources. To the classic ones, axial dispersion, eddy diffusion, and mass transfer resistances, it has become classic to add one originating from extra column sources (e.g., detector response time, injection volume, connecting tubes). This work shows that the radial heterogeneity of the column bed is another such source of band broadening, long neglected.

Distribution of the Analyte Concentration

The ideal injection profile for any chromatographic system would be a rectangular band having a constant concentration throughout its entire volume. The representation of this band in concentration-time coordinates corresponds to a pulse function of constant height equal to the injected sample concentration and a width determined by the injection volume and the mobile phase flow rate. In the present study, this band should be narrow compared to the retention volume of the solute. However, any experimental injection profile differs somewhat from this ideal model, by the lack of a concentration plateau, at least for analytical-size injection volumes, and by diffused sides which, in favorable circumstances, are intermediate between error functions and a Gaussian profile. We showed in a previous work (Farkas et al., 1994) that the concentration signals recorded at different locations spread over the inlet cross section of an analytical-size column have narrow, quasi-simultaneous Gaussian profiles. The homogeneous distribution of the injected sample across the inlet cross section of the column was demonstrated for the axial compression column (see "Experimental" section). Further proof is brought by the radial distribution of the eluted amounts. Integration of the concentration histories afforded by each sensor gives the local mass of analyte eluted per unit surface area of the column cross section. A plot of this density vs. the radial position is given in Figure 7. It shows a nearly constant density of the eluted band, although a slightly larger amount of feed may be eluting from the peripheral region of the column than from the core region, a trend not found for the injection data in Table I. The radial distribution of the maximum peak concentration (not shown) is much flatter for the second column than for the first one (Figure 8a). This result would not be obtained without a homogeneous distribution of the injected band. This result is certainly a tribute to the distributor designers.

The peaks recorded at different locations over the outlet cross section of the column during one single run are shown in Figure 8a as concentration profiles. They differ signifi-

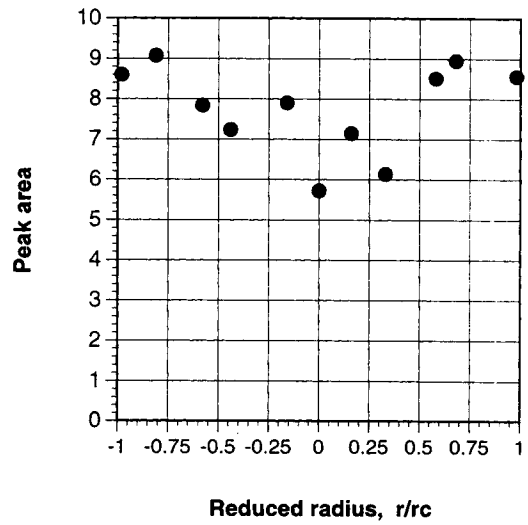

Figure 7. Radial distribution of local density of eluted analyte.

The corresponding data are obtained by integration of the concentration histories in Figure 8a.

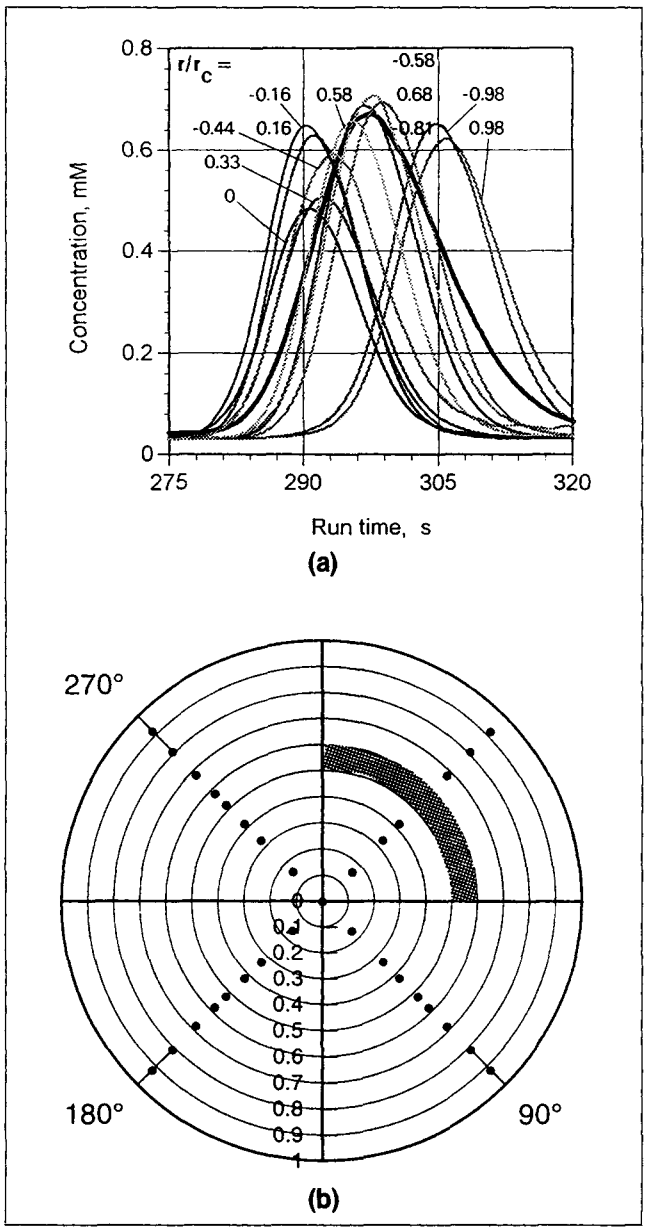

Figure 8. (*a*) Normalized and base-line corrected peaks, recorded during the same run at 11 different locations over the column cross section, overlaid.

The solid line is the reconstructed peak (see also Figure 9): (*b*) Partitioning of the cross-sectional area and location of the detection for each sector used in reconstructing the overall peak from individual peaks recorded in parallel.

cantly in timing (see mobile phase velocity), in bandwidth (see efficiency), and slightly in band shape. The important differences observed in peak heights for the raw data was largely due to the different response factors of the optical-fiber assemblies and amplification factors of the corresponding diodes, differences that are easily corrected by proper calibration (Farkas et al., 1994, 1996). A discussion of the many parameters affecting the specific response of an optical-fiber assembly-diode couple can be found in our previous article (Farkas et al., 1996). The more important ones in the present case seem to be the fiber assembly geometry and photodiode aging. In order to compensate for these differences, calibration was performed by calculating response factors as the ratios of the plateau heights obtained for each sensor during a staircase breakthrough experiment. In a breakthrough experiment, the composition of the whole effluent eventually becomes homogeneous, given enough run time, even if the packing is heterogeneous. The base-line corrected, parallel, concentration chromatograms eluted during one run shown in Figure 8a differ in heights, widths, and retention times.

From the previous results on the distribution of mobile phase velocities and local efficiencies, one would expect that the spatial distribution of the analyte molecule density (i.e., of the analyte concentration profiles) within the component zone includes the following features. The concentration histories recorded at different points in the central region of the column exit are more or less evenly dispersed, and they all move at nearly the same velocity along parallel stream paths. In the external region, these concentration histories are more diffuse, exhibiting lower maxima, according to the distribution of the local efficiency. They migrate more slowly in the region closer to the column wall and their elutions are shifted in time, according to the uneven flow profile induced by the bed heterogeneity. The experimental results show a somewhat different picture (Figure 8a). The results agree well with the prediction as far as the distribution of average residence times is concerned. However, the distribution of the concentration maxima is not even along any portion of the column diameter, including the central core region. The maximum concentration of the bands is smaller at the column center than in the region surrounding it. As expected, it also becomes smaller close to the column wall. That this observation is not an experimental artifact is suggested by the fact that the concentration maxima of the local histories vary smoothly along any column diameter. Note that peaks recorded at the same or nearby locations with different sensors are close in height, while peaks recorded at the intermediate locations with different sensors are intermediate in height. Analytical columns previously studied with different experimental setup, using either electrochemical or fluorescence detection systems, showed similar trends.

Determination of the bulk elution peak from local peaks

The set of local data acquired and discussed in the preceding allows a detailed discussion of the profile of the bands obtained with a conventional on-line detector working with the bulk eluent. All the volume elements that are part of the analyte band and elute earliest contribute to the peak front. The central part of the peak is recorded during the elution of the volume elements that are at the periphery of the central core region of the column (Figure 8a). However, the analyte concentration in the region close to the column wall begins to build up only when the concentration in the core region of the bed has peaked and is already decreasing (Figure 8a). Note in Figure 8a that the "resolution" between the peaks at the column center and at a relative radius of 0.98 is nearly unity! The rear part of the peak is made of molecules eluting close to the column wall, at a time when most of the other molecules have left the column. Thus, molecules eluting early build up the peak front, while those lagging behind the bulk,

in the region close to the wall, are responsible for the apparent tailing of the peak recorded by a detector operating on the bulk eluent. To the three conventional sources of tailing in chromatography—a tailing injection profile, too slow a detector response, and heterogeneous mass transfer kinetics—we must now add a fourth one—the effect of an uneven radial distribution of the flow velocity, causing molecules to move at different average velocities in different regions of the column cross section.

Finally, the reconstruction of the overall peak profile obtained with a conventional detector offers a check of the consistency of all the experimental results reported here. This profile is obtained by summing up the contributions of all the slices shown in Figure 8b. Each contribution is calculated as the product of the concentration profile (Figure 8a) recorded by the sensor labeled in Figure 8b and the fractional area of the slice. The concentric segments of annuli in Figure 8b were arranged in such a way that each one contains at least one location where detection has been performed (Figure 8a). When there are two sensors in a slice, the average profile is taken. For the few sectors that did not contain such a location, the value interpolated from neighboring sectors was used. The result of this calculation was the profile represented by the thick solid line shown in Figure 8a. This peak is centered at the weight center of the set of locally recorded peaks that were used to generate it. Its shape reflects the contributions from all these peaks. Note that its tailing is much more important than that of any local profile. Next, this calculated peak profile is compared to the profile recorded when the column was tested in a standard instrumental setup (Sarker and Guiochon, 1995a,b), following packing and bed stabilization. Figure 9 shows that both the envelope and the experimental peak profile overlay fairly well, except for a shift in their retention time. This shift is fully accounted for by the postcolumn dead volume of the connecting tube now required between the column outlet and the detector. This volume could have been subtracted but was not because otherwise the two peaks would be difficult to distinguish. The experimental peak tails slightly more than the reconstructed one, probably a result of the impossibility of recording any profile closer to the wall than the profile at $r/r_c = 0.98$, or closer than 0.5mm.

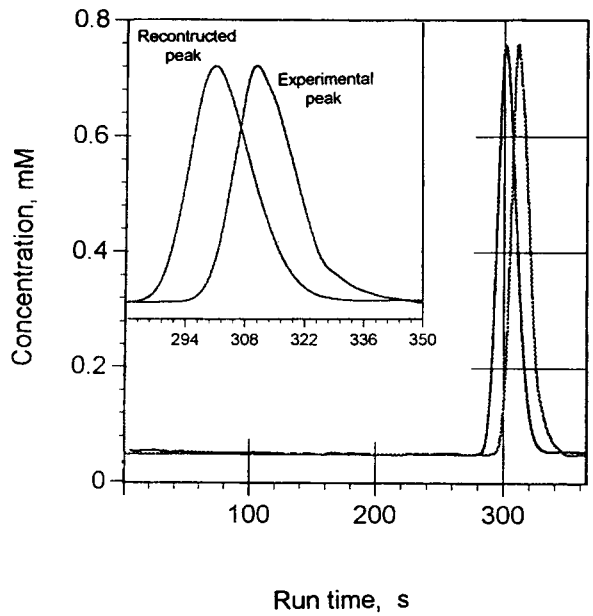

Figure 9. Reconstructed and experimental peak, overlaid.

Conclusions

Like analytical-scale chromatographic columns, preparative-scale columns exhibit significant cross-column variations of the local average flow velocity, the local column efficiency, and the local analyte concentration. Inside a central core region with a diameter on the order of two-thirds the column diameter, the velocity is nearly constant. In the external region, the velocity decreases with decreasing distance to the column wall. Both regions occupy comparable fractions of the column volume. However, there is no clear boundary between these two regions. The local column efficiency is everywhere higher than the overall efficiency determined with an on-line conventional detector. It varies across the column section, and is higher in the central core region; in the external region, it decreases with decreasing distance to the column wall where it is at least 30% lower than in the column center.

The consequence of this heterogeneous behavior of the column is that the conventional elution profile is a complex convolution of the convection and dispersion phenomena taking place in the chromatographic column. This profile is not a simple consequence of the local axial dispersion and of the mass-transfer phenomena taking place in the column, but is influenced by the heterogeneity of the column used. It has long been observed that chromatographic peaks tail more than can be explained by most models. Our results demonstrate that this tailing is mainly caused by the uneven distribution of the local velocities. The fact that the fraction of the analyte that migrates close to the column wall does so at a lower linear velocity than the fraction that migrates in the core region is responsible for most of the observed peak tailing. Obviously, two space coordinates, the column length and its radius, and not only the former, are needed in a realistic model of chromatography (Yun and Guiochon, 1994, 1996), unless the contribution of the uneven radial distribution of the flow velocity is lumped into the mass-transfer coefficient of a lumped kinetic model.

The origin of the column heterogeneity described in this work was discussed recently (Guiochon et al., 1997). It is most probably related to the interaction between the relatively high compressibility of pulverulent materials (Guiochon and Sarker, 1995; Sarker et al., 1996; Taylor, 1948) and the complex distribution of stress during the compression of the packing. The latter was abundantly illustrated by Train (1956, 1957, 1960) using an experimental setup nearly identical to an axial compression column.

Acknowledgments

This work has been supported in part by Grant DE-FG05-88ER13859 of the Department of Energy and in part by the cooperative agreement between the University of Tennessee and the Oak Ridge National Laboratory. We thank Klaus Lohse (BTR Separations, Wilmington, DE) for the generous gift of the stationary phase used.

Literature Cited

Baumeister, E., U. Klose, K. Albert, E. Bayer, and G. Guiochon, "Determination of the Apparent Transverse and Axial Dispersion Coefficients in a Chromatographic Column by Pulsed Field Gradient Nuclear Magnetic Resonance," *J. Chromatog. A*, **694**, 321 (1995).

Baur, J. E., E. W. Kristensen, and P. M. Wightman, "Radial Dispersion from Commercial High-Performance Liquid Chromatography Columns Investigated with Microvoltammetric Electrodes," *Anal. Chem.*, **60**, 2334 (1988).

Baur, J. E., and P. M. Wightman, "Microcylinder Electrodes as Sensitive Detectors for High-Efficiency, High-Speed Liquid Chromatography," *J. Chromatog.*, **482**, 65 (1989).

Bayer, E., E. Baumeister, U. Tallarek, K. Albert, and G. Guiochon, "NMR Imaging of the Chromatographic Process. Deposition and Removal of Gadolinium ions on a Reversed-Phase Liquid Chromatographic Columns, " *J. Chromatog. A*, **704**, 37 (1995).

Collins, R. E., "Flow through Porous Materials," Reinhold, New York, NY p. 47 (1961).

Ebach, E. A., and R. R. White, "Mixing of Fluids through Beds of Packed Solids," *AIChE J.*, **4**, 161 (1958).

Eon, C. H., "Comparison of Broadening Patterns in Regular and Radially Compressed Large-Diameter Columns," *J. Chromatog.*, **149**, 29 (1978).

Farkas, T., J. Q. Chambers, G. Guiochon, "Column Efficiency and Radial Homogeneity in Liquid Chromatography," *J. Chromatog.*, **679**, 231(1994).

Farkas, T., M. J. Sepaniak, and G. Guiochon, "Column Radial Homogeneity in HPLC," *J Chromatog.*, **740**, 169 (1996).

Giddings, J. C., "Principles of Column Performance in Large Scale Gas Chromatography," *J. Gas Chromatog.*, **1**(1), 12 (1963).

Giddings, J. C., *Dynamics of Chromatography, Part I: Principles and Theory*, Marcel Dekker, New York, NY, p. 195, (1965).

Giddings, J. C., *Unified Separation Science*, Wiley, New York, NY, p. 62, (1991).

Guan, H., G. Guiochon, D. Coffey, E. Davis, K. Gulakowski, and D. W. Smith., "Study of Physico-Chemical Properties of Some Packing Materials," *J. Chromatog. A*, **736**, 21 (1996).

Guiochon, G., T. Farkas, H. Guan-Sajonz, J. Koh, M. Sarker, B. Stanley, and T. Yun, "The Consolidation of Particles and the Packing of Chromatographic Columns," *J. Chromatog. A*, **762**, 83 (1997).

Guiochon, G., M. Sarker, "Consolidation of the Packing Material in Chromatographic Columns under Dynamic Axial Compression: I. Fundamental Study," *J. Chromatog. A*, **704**, 247 (1995).

Guiochon, G., S. G. Shirazi, and A. M. Katti, *Fundamentals of Preparative and Nonlinear Chromatography*, Academic Press, Boston, MA (1994).

Gunn, D. J., "Theory of Axial and Radial Dispersion in Packed Bed," *Trans. Inst. Chem. Eng.*, **47**, T351 (1969).

Gunn, D. J., "Mixing in Packed and Fluidised Beds," *Chem. Eng.*, **46**, CE153 (1968).

Hiby, J. W., Interaction between Fluids and Particles, P. A. Rottenburg, Ed., Inst. of Chem. Engs., London, p. 312 (1962).

Horne, D. S., J. H. Knox, and L. McLaren, "A Comparison of Mobile Phase Peak Dispersion in Gas and Liquid Chromatography," *Sep. Sci. Technol.*, **1**, 531 (1966).

Kamiński, M., "Simple Test for the Determination of the Degree of Distortion of the Liquid-Phase Flow Profile in Columns for Preparative Liquid Chromatography," *J. Chromatog.*, **589**, 61 (1992).

Karger, B., L. Snyder, and Cs. Horváth, *An Introduction to Separation Science*, Wiley, New York, p. 90 (1973).

Knox, J. H., G. R. Laird, and P. A. Raven, "Interaction of Radial and Axial Dispersion in Liquid Chromatography in Relation to the 'Infinite Diameter Effect'," *J. Chromatog.*, **122**, 129 (1976).

Knox, J. H., and J. F. Parcher, "Effect of Column to Particle Diameter Ratio on Dispersion of Unsorbed Solutes in Chromatography," *Anal. Chem.*, **41**, 1599 (1969).

Peters, D. G., J. M. Hayes, and G. M. Hieftje, *Chemical Separations and Measurements*,, Saunders Golden Sunburst Series, Philadelphia, PA, p. 531 (1974).

Poole, C. F., and S. K. Poole, *Chromatography Today*, 2nd ed., Elsevier, Amsterdam (1993).

Sarker, M., and G. Guiochon, "Study of the Packing Behavior of Axial Compression Columns for Preparative Chromatography," *J. Chromatog. A*, **702**, 27 (1995a).

Sarker, M., and G. Guiochon, "Study of the Operating Conditions of Axial Compression Columns for Preparative Chromatography," *J. Chromatog. A*, **709**, 227 (1995b).

Sarker, M., A. M. Katti, and G. Guiochon, "Consolidation of the Packing Material in Chromatographic Columns under Dynamic Axial Compression: II. Consolidation and Breakage of Several Packing Materials," *J. Chromatog. A*, **719**, 275 (1996).

Scheidegger, A. E., *The Physics of Flow in Porous Media*, Univ. of Toronto Press, Toronto, Canada, p.126, (1974).

Tallarek, U., K. Albert, E. Bayer, and G. Guiochon, "Measurement of Transverse and Axial Apparent Dispersion Coefficients in Packed Beds by PFGNMR," *AIChE J.*, **42**, 3041 (1996).

Tallarek, U., E. Baumeister, K. Albert, E. Bayer, and G. Guiochon, "NMR Imaging of the Chromatographic Process. Migration and Separation of Bands of Gadolinium Chelates," *J. Chromatog. A*, **696**, 1 (1995).

Taylor, D. W., "Fundamentals of Soil Mechanics," Wiley, New York (1948).

Train, D., "An Investigation Into the Compaction of Powders", *J. Pharm. Pharmacol.*, **8**, 745 (1956).

Train, D., "Transmission of Forces Through a Powder Mass during the Process of Pelleting," *Trans. Instn. Chem. Engrs.*, **35**, 258 (1957).

Train, D., and J. A. Hearsey, "The Use of Laminar Lubricants in Compaction Processes," *J. Pharm. Pharmacol.*, **12**, 97T (1960).

Yun, T., and G. Guiochon, "Visualization of Column Packing Heterogeneity," *J. Chromatogr. A*, **760**, 17 (1997).

Yun, T., and G. Guiochon, "Modeling of Radial Heterogeneity in Chromatographic Columns: Columns with Cylindrical Symmetry and Ideal Model," *J. Chromatog. A*, **672**, 1 (1994).

Yun, T., and G. Guiochon, "Modeling of Radial Heterogeneity in Chromatographic Columns: II. Separation of a Two-Component Mixture on a Column with Cylindrical Symmetry," *J. Chromatog. A*, **734**, 97 (1996).

Manuscript received Nov. 15, 1996, and revision received Apr. 24, 1997.